International Journal of Fluid Power 4 (2003) No. 2 pp. 5-14

DEVELOPMENT OF A QUIETER VARIABLE-DISPLACEMENT VANE PUMP FOR AUTOMOTIVE HYDRAULIC POWER STEERING SYSTEM

Eiichi Kojima

Department of Mechanical Engineering, Kanagawa University, 3-27-1, Rokkakubashi, Kanagawa-ku, Yokohama, Japan
kojime01@kanagawa-u.ac.jp

Abstract

In an automotive hydraulic power steering system a variable-displacement vane pump that is equipped with a control device for adjusting the eccentricity of the cam ring and thus pump delivery flow rate according to the pump rotational speed (i.e. vehicle speed) is gradually being used for energy saving in place of a fixed-displacement vane pump. However, fluid-borne noise radiating into the passenger compartment has greatly increased following this replacement, and, therefore, countermeasures to reduce pump source flow ripple have been required more than anything else to further spread its usage. This paper reports on development research of a quieter (low fluid-borne noise level) variable-displacement vane pump for HPS systems. First, it is indicated based on both experimental measurements and simulation analysis of pump source flow ripple that the excessive increase of fluid-borne noise produced by existing variable-displacement vane pumps equipped with a cylindrical cam ring is mainly caused by vane bounce occurring in the trapping sections near the bottom dead center, which is difficult to prevent when a conventional cylindrical (completely round profile) cam ring is used. Next, a new cam ring profile for preventing vane bounce called a "modified profile cam ring" is proposed and its effectiveness is examined by noise tests in the passenger compartment of a real car as well as measurements of pump source flow ripple in a bench test circuit. The proposed cam ring is found to be successful in reducing fluid-borne noise to at least the level of a fixed pump. The newly developed types of pumps have already been put into practice in several kinds of automobiles.

Keywords: automotive hydraulic power steering, variable-displacement vane pump, fluid-borne noise, pressure pulsation, vane bounce

1 Introduction

In recent years, in an automotive hydraulic power steering (HPS) system, a variable-displacement vane pump, which is equipped with a control device for adjusting the eccentricity of the cam ring and thus pump delivery flow rate according to the pump rotational speed (i.e. vehicle speed), is gradually being used for energy saving in place of a fixed-displacement vane pump. However, fluid-borne noise radiating into the passenger compartment has greatly increased following this replacement, and, therefore, countermeasures to reduce flow ripple from the pump source have been required more than anything else to further spread its usage.

The objective of this research is the development of a variable-displacement vane pump for HPS system, which can reduce fluid-borne noise in a passenger compartment to at least the level of a fixed-displacement vane pump without vast changes for the mechanism. For this purpose, in advance of development research, the excessive increase in vibration and noise by the existing variable-displacement vane pump, which is equipped with a conventional cylindrical (completely round profile) cam ring was resolved by both experimental measurements and simulation analysis of pump source flow ripple, together with the measurement of pump casing vibration and nearby noise.

In regard to the vibration and noise generated by a fixed-displacement vane pump for HPS system, research has been reported on the analysis of pump source flow ripple and source impedance by both experimental measurements and simulations (Dickinson et al, 1993), examination of repeatability, reproducibility and production variability in measured values of pump source flow ripple and source impedance based on the ISO standard (Qatu et al, 1999), examination of the influence of design tolerance on noise, vibration and harshness by binaural measurement and jury evaluation (Fernholt and Bishop, 1999), and the automated production noise testing (Bleitz et al, 1997). In regard to the vibration and noise of a variable-displacement vane pump for HPS

This manuscript was received on 27 February 2003 and was accepted after revision for publication on 28 April 2003

system, however, detailed research has not been reported so far as the author knows, though there has been research investigating the dynamics of such a pump (Karmel, 1986).

In this paper, a new cam ring with a special internal profile called a "modified profile cam ring" (MPCR) for preventing vane bounce (referred to as "vane-alienation") is proposed. Its effectiveness is examined by noise testing in the passenger compartment of a real car as well as experimental measurements of pump source flow ripple (and pump casing vibration and nearby noise) in a bench test circuit under a wide range of operating conditions, particularly pump rotational speed and load (delivery) pressure.

2 Source Flow Ripple and Vane Bounce of Variable-Displacement Vane Pump Equipped with a Cylindrical Cam Ring

The pump chosen as the subject of study for design improvement is a variable displacement vane pump that is equipped with a control device for adjusting the eccentricity of the cam ring (and thus the pump delivery flow rate) according to pump rotational speed (i.e. vehicle speed). Figure 1 shows a schematic diagram explaining the mechanism of the investigated pump (maximum displacement: 9.6 cm^3/rev, number of vanes: 11).

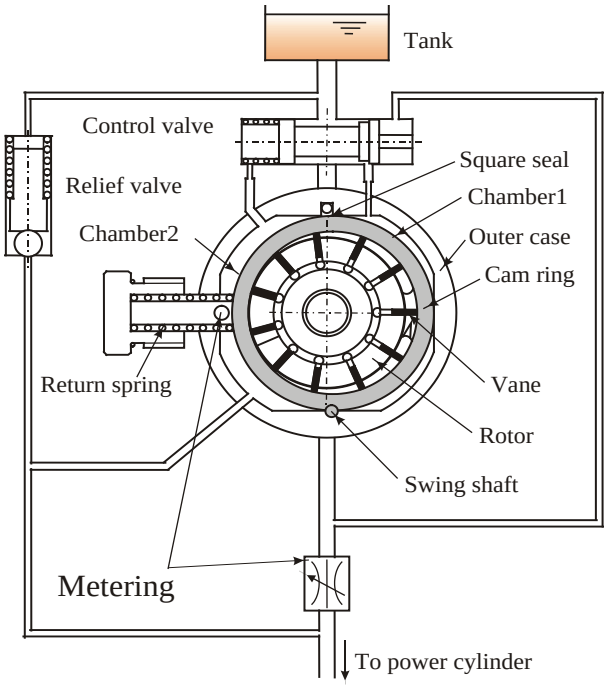

Fig. 1: *Schematic diagram of power steering variable-displacement vane pump used in this study*

Figure 2 and 3 show the measured time-history waveforms and amplitude spectra of pump source flow ripple, respectively, produced by an existing variable-displacement vane pump equipped with a cylindrical cam ring obtained by the author's proposed method called the "two pressures/two systems" method (Kojima, 1992; Kojima and Yu, 2000), where θ of the x coordinate axis in Fig. 2 expresses the angle of the center position between two adjacent vanes from the bottom dead center. Simulation results from the mathematical model that neglects vane bounce (see Appendix) are also indicated in these figures.

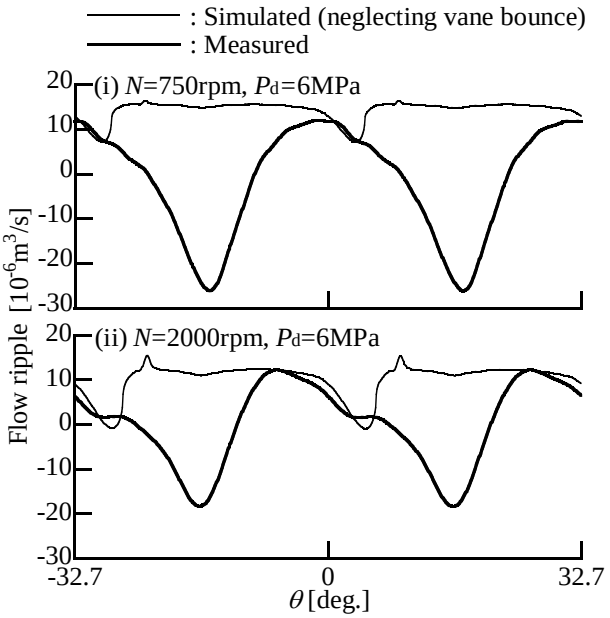

Fig. 2: *Measured and simulated (neglecting vane bounce) time-history waveforms of source flow ripple produced by a variable-displacement vane pump equipped with a cylindrical cam ring*

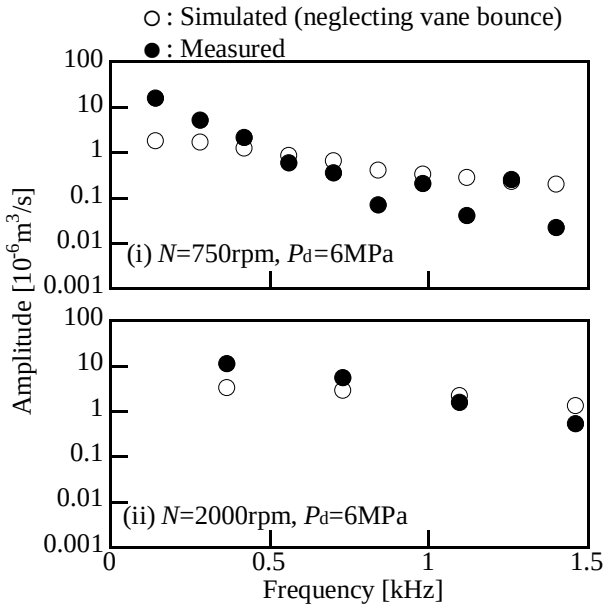

Fig. 3: *Measured and simulated (neglecting vane bounce) amplitude spectra of source flow ripple produced by a variable-displacement vane pump equipped with a cylindrical cam ring*

Figure 4 and 5 show the measured time-history waveforms and amplitude spectra of pump source flow ripple, respectively, produced by a fixed-displacement vane pump (displacement: 10 cm^3/rev, number of vanes: 10) for an existing HPS system, which were obtained for the purpose of comparing with those of the proposed variable vane pump. The repeatability of measurements (1st-3rd) is also indicated in these figures.

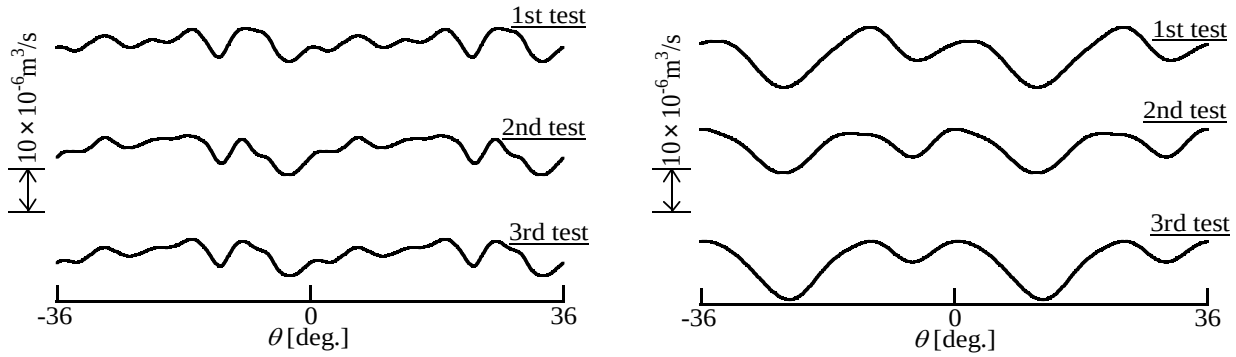

(i) N = 750 rpm, P_d = 6 MPa *(ii) N = 2000 rpm, P_d = 6 MPa*

Fig. 4: *Measured time-history waveforms of source flow ripple produced by a fixed-displacement vane pump and their repeatability*

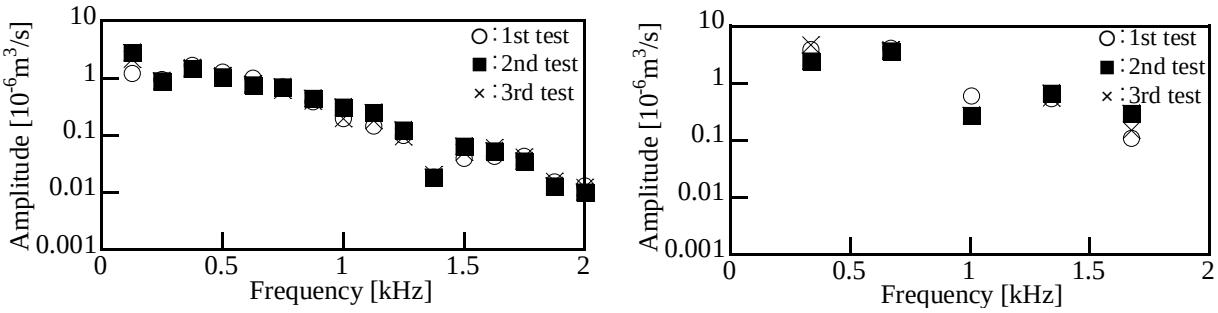

(i) N = 750 rpm, P_d = 6 MPa *(ii) N = 2000 rpm, P_d = 6 MPa*

Fig. 5: *Measured amplitude spectra of source flow ripple produced by a fixed-displacement vane pump and their repeatability*

It can be seen from Fig. 2 to 5 that the intermittent unsteady leakage generated in the variable-displacement vane pump is considerably large compared to that of the fixed-displacement vane pump (especially, in low-speed /high-pressure operation). It can also be seen that this leakage happens in almost all regions of the trapping section and maximizes when a vane comes near to the bottom dead center. Furthermore, it is well known that, in a piston pump, for instance, where the movement of pumping elements is mechanically restricted to stay within clearances, the simulation results of source flow ripple agree with the experimental measurements within an uncertainty of 20-30% for the most part (Kojima et al, 2000). For the variable-displacement pump tested, however, the difference between simulation results (neglecting vane bounce) and experimental measurements is large (5-6 times for peak-peak values).

From these experimental facts, it can be inferred that the excessive increase in pump source flow ripple produced by the variable-displacement vane pump equipped with a cylindrical cam ring is dominantly caused by the increase in unsteady leakage flow rate from the clearance of vane tip due to the vane bounce.

3 Proposal of New Cam Ring for Preventing Vane Bounce

To identify the cause of vane bounce and then think of countermeasures against it, in the early stage of research, pump source flow ripple was measured systematically changing the port angles (pre-compression and pre-expansion angle), dimensions and shapes of relief grooves, configuration of back pressure grooves, etc. But, it was found that in as far as the cylindrical cam ring was used, these countermeasures were all ineffective and even exhibited a contrary effect in some cases. From these experimental facts (results are omitted) and the experimental results shown in Fig. 2, it can be concluded that the occurrence of vane bounce is strongly influenced by the interior profile of the cam ring as follows. The vane positioned in the trapping section near the bottom dead center "for instance" is subjected to delivery pressure on the front face and suction pressure on the rear face, that is, an unbalanced force is applied on the vane and thus the vane may be stuck at the corner of vane slot as shown in Fig. 6. Thereby, the vane cannot be pushed up to the position, where the vane tip contacts the inner surface of the cam ring, only by centrifugal force and back pressure force. Thus, the vane bounce occurs in sections where the radius of the vane must increase with the increase in the rotational angle of the rotor (i.e., in the first half of the trapping section near the bottom dead center and the latter half of the trapping section near the top dead center).

The dotted lines in Fig. 7 show the pump source flow ripple calculated from a mathematical model taking the leakage from the vane tip clearance into consideration, together with the measured results represented by the solid lines. It is assumed that the vane begins to stick and

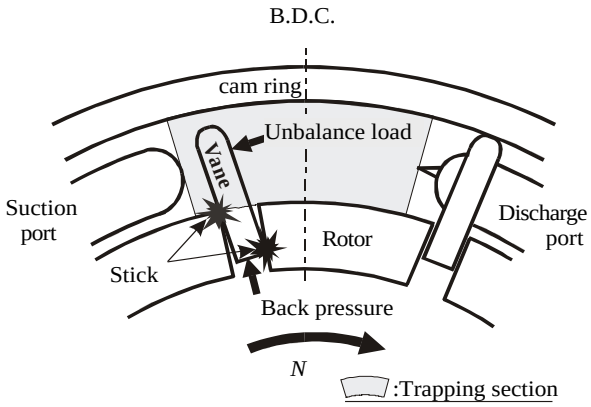

Fig. 6: *Schematic illustration showing the generation mechanism of vane bounce*

then separate from the inner surface of the cam ring from the angular position just after the beginning of trapping section near the bottom dead center (to be more precise, at $\theta = 6^0$). It can be seen from these results that close agreement between measured and simulated values is obtained except that high frequency components appeared in the simulation results. From the above investigations, it could be verified that this supposition for the generation mechanism of vane bounce was appropriate, although it is an indirect verification.

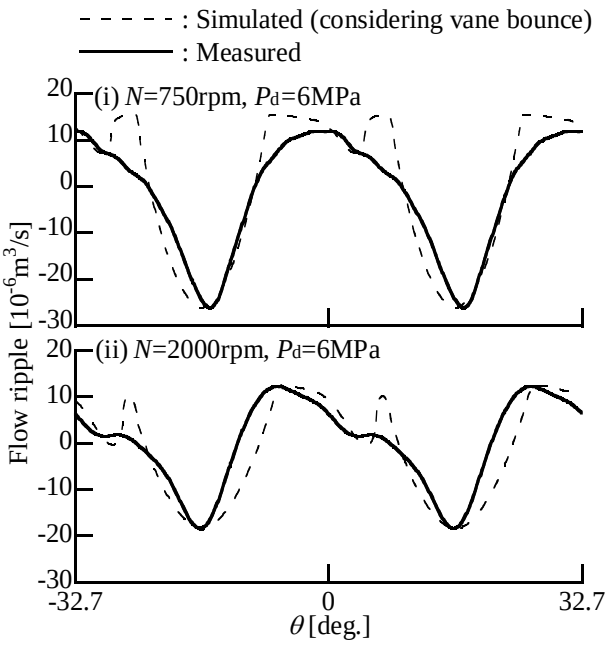

Fig. 7: *Simulated (considering vane bounce) and measured time-history waveforms of source flow ripple produced by a variable-displacement vane pump equipped with a cylindrical cam ring*

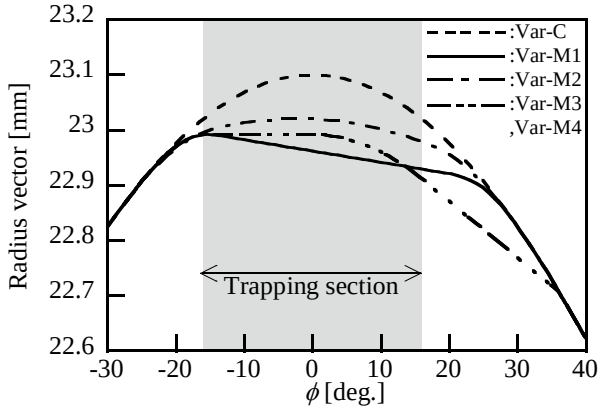

(a) Nearby bottom dead center

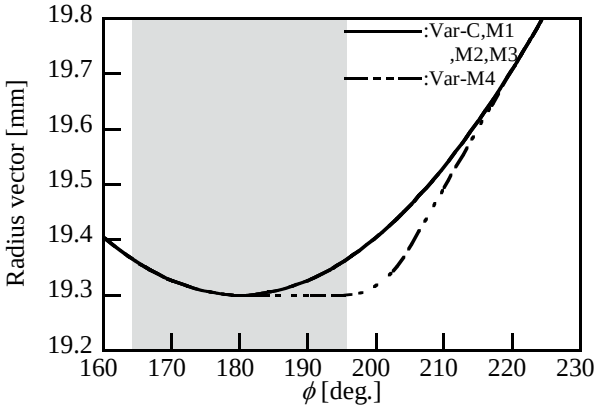

(b) Nearby top dead center

*(i) At the time of low speed operation (*e *= 1.9 mm)*

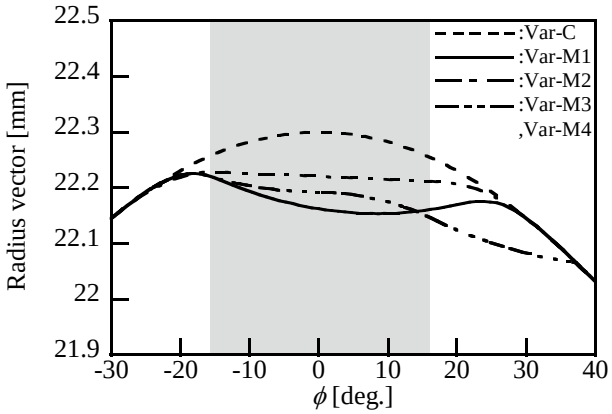

(a) Nearby bottom dead center r

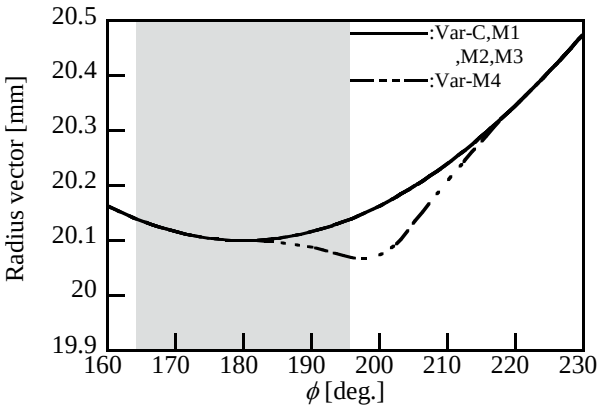

(b) Nearby top dead center

*(ii) At the time of high speed operation (*e *= 1.1mm)*

Fig. 8: *Radius vectors of the proposed modified profile cam rings (Var-M1 - Var-M4) at trapping sections*

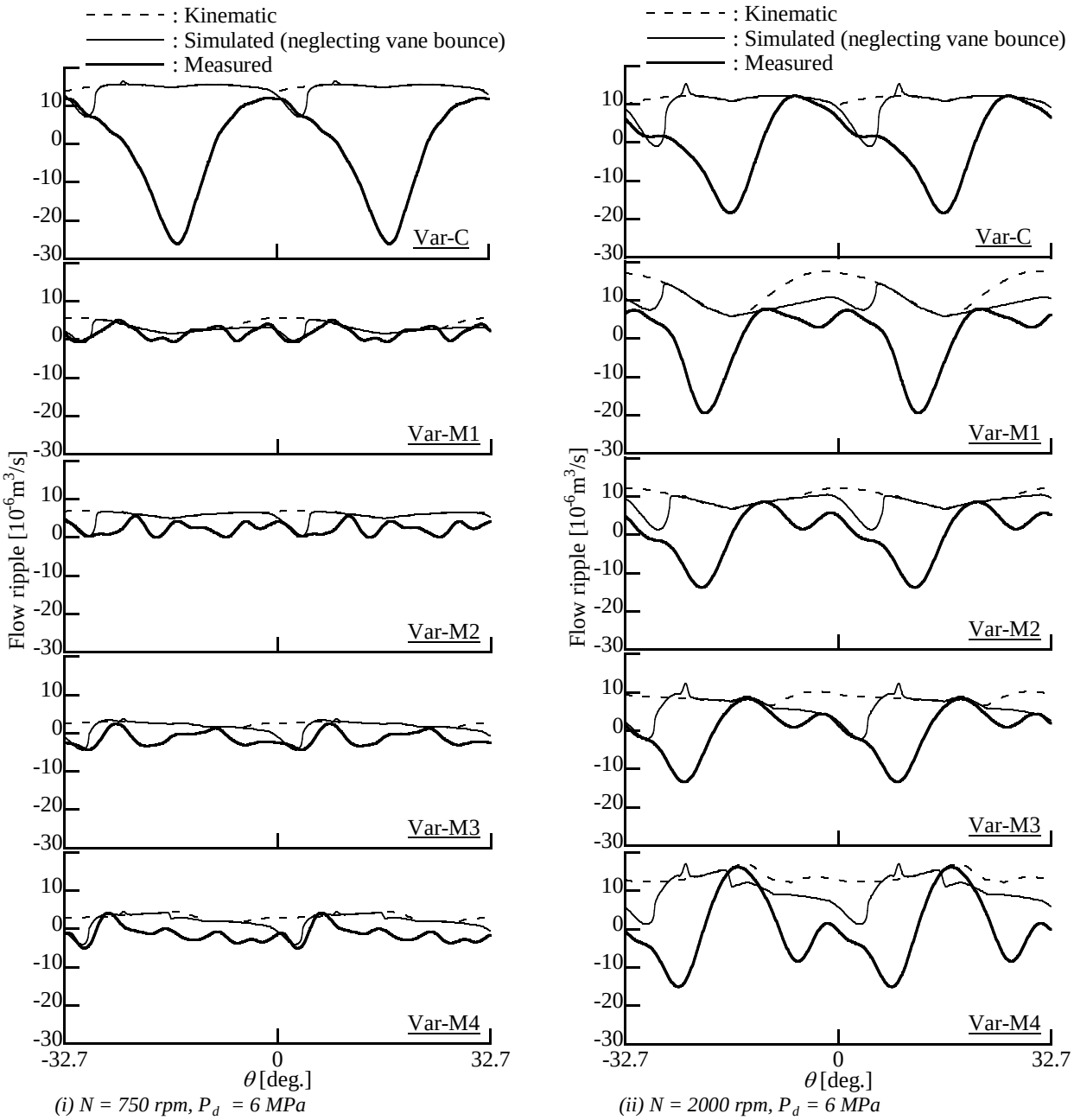

Fig. 9 : *Comparison of measured time-history waveform of source flow ripple between various cam ring profiles*

On the basis of the above considerations, cam rings of various profiles were designed and manufactured under the following conditions 1. – 4., so that the radius vector of the vane does not need increasing with the increase in the rotational angle of the rotor in the trapping section where an unbalanced load is applied on the vane.

1. The gradient of the radius vector of the vane to the rotational angle of the rotor is negative in any angular position in the trapping section near the bottom dead center in low-speed operation (e = 1.9 mm) (hereafter, "Var-M1")
2. The gradient of the radius vector of the vane to the rotational angle of the rotor is negative in any angular position in the trapping section near the bottom dead center in high-speed operation (e = 1.1 mm) ("Var-M2").
3. The gradient of the radius vector of the vane to the rotational angle of the rotor is negative in any angular position in the trapping section near the bottom dead center regardless of pump revolution speed ("Var-M3").
4. The gradient of the radius vector of the vane to the rotational angle of the rotor is negative in any angular position in both trapping sections near the bottom and top dead center regardless of pump revolution speed ("Var-M4").

Provided that the negative gradient curve of the radius vector in the trapping section/sections was connected smoothly to the cylindrical curve outside the trapping section by a high-order curve.

Figure 8 shows the curve of the radius vector of the MPCR near the bottom and top dead center, where θ in the horizontal axis indicates the rotational angle of the

vane based on the bottom dead center.

In this study, the industrial usefulness of the proposed modified profile cam ring is examined by measuring both the pump source flow ripple (and pressure ripple) and the audible noise in the passenger compartment of a real car generated by the variable-displacement vane pump equipped with the above cam ring.

4 Pump Source Flow Ripple Generated by Variable-displacement Vane Pump Equipped with "Modified Profile Cam Ring"

Figure 9 and 10 show the measured time-history waveforms and amplitude spectra of pump source flow ripple generated by the variable-displacement vane pump equipped with the cam rings of Var-M - Var-M4, respectively, together with that of the conventional pump equipped with a cylindrical cam ring (Var-C). (i) is for an operating condition of low-speed/high-pressure (N = 750 rpm, P_d = 6 MPa) and (ii) for an operating condition of high-speed/high-pressure (N = 2000 rpm, P_d = 6 MPa). Simulation results of the actual source flow ripple and the theoretical source flow ripple due only to pumping mechanism, which was calculated from the mathematical model (shown in Appendix) that neglects vane bounce, are also indicated in these figures. Figure 11 shows the measured overall value (sum of the harmonic amplitude up to 2 kHz) of the source flow ripple generated by the Var-M1-Var-M4 vane pumps, together with those of the fixed-displacement vane pump and the Var-C pump. The test conditions of low-speed/low-pressure (N = 750 rpm, P_d = 1 MPa), low-speed/high-pressure (N = 750 rpm, P_d = 6 MPa), high-speed/low-pressure (N = 2000 rpm, P_d = 1 MPa) and high-speed/high-pressure (N = 2000 rpm, P_d = 6 MPa) correspond to the driving conditions of idling, parking, steady state driving and driving around corners in town, respectively.

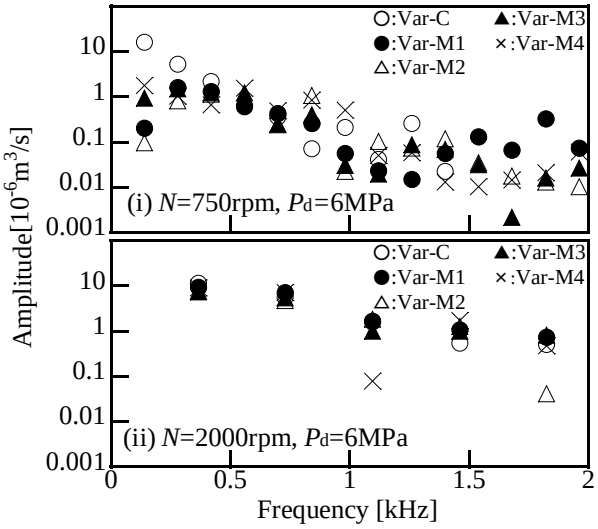

Fig. 10: *Comparison of measured amplitude spectra of source flow ripple between various cam ring profiles*

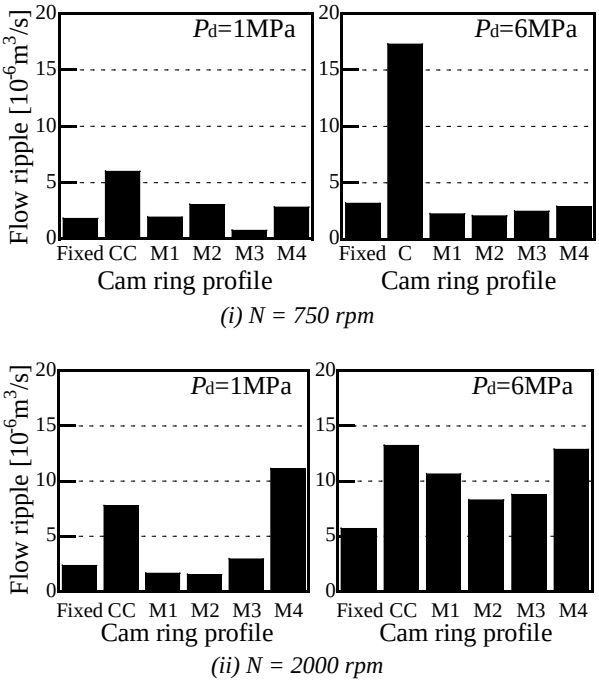

Fig. 11: *Comparison of measured overall values of source flow ripple between various cam ring profiles*

It can be seen from these results that the variable-displacement vane pump equipped with the proposed MPCR has the following characteristics.

- Pump source flow ripple can be reduced dramatically in low-speed operation compared to the Var-C pump because vane bounce is almost prevented under this condition.
- Pump source flow ripple can be reduced at least to the level of a fixed type vane pump except in high-speed/high-pressure operation.
- Pump source flow ripple of the Var-M1 - Var-M3 pumps excluding the Var-M4 pump has qualitatively the same characteristics as the design concept indicated in Section 3.
- Since vane bounce cannot be prevented satisfactorily in high-speed/high-pressure operation, the reduction in source flow ripple is only 20 - 30% compared to the Var-C pump.
- The Var-M4 pump, whose radius vector of the vane is designed for a negative gradient curve near the top dead center as well as the bottom dead center, inversely increases the source flow ripple in high-speed operation (the clear cause of this phenomenon has not been identified).

From these tests, it was verified that, if the curve of the radius vector of the vane was designed appropriately, the pump source flow ripple that caused fluid-borne noise could be reduced to at least the level of a fixed-displacement pump. Besides, it has been confirmed that the audible noise radiated directly from the pump casing can also be reduced to the level of the fixed type vane pump, but the details are omitted because of limitations on the length of this paper.

5 Effect of "Modified Profile Cam Ring" on Reduction of Noise in Passenger Compartment

In order to consider the feasibility of a variable-displacement vane pump equipped with the proposed MPCR, its effectiveness on the reduction of noise in the passenger compartment of a real car was examined by installing it in a hydraulic power steering system. The sound pressure level and sound pressure spectra in the center of the passenger compartment (close to the driver's ears) and the pressure ripple at the pump exit were measured for the Var-M3, Var-C and fixed pumps. Oil temperature was kept at a constant value of around 70°C during tests.

Table 1 shows the measured overall value and fundamental component of A-weighted sound pressure level for the fixed, Var-C and Var-M3 pumps under the operating conditions of low pressure (P_d = 0.7 MPa) and high pressure (P_d = 5.4 MPa), respectively, for both the low-speed (N = 920 rpm) and high-speed (N = 2000 rpm) conditions. Figure 12 shows an example of the spectra of the A-weighted sound pressure level of the above three pumps. Table 2 shows an overall value and fundamental component of pressure ripple at the pump exit measured simultaneously with sound pressure, provided that the pressure ripple is expressed in a dB unit relative to 0.1 MPa.

Table 1: Overall value and fundamental component of A-weighted sound pressure level in a passenger compartment

			Low speed (920 rpm)			High speed (2.000 rpm)		
			Fixed	Var-C	Var-M3	Fixed	Var-C	Var-M3
Sound pressure level[dB(A)]	Overall	Low pressure (0.7 MPa)	40.9	42.9	41.3	44.5	45.3	45.0
		High pressure (5.4 MPa)	42.2	44.5	42.9	47.0	45.7	44.7
	Fundamental	Low pressure (0.7 MPa)	12.6	20.2	8.3	29.6	27.5	28.5
		High pressure (5.4 MPa)	20.5	36.8	18.3	37.9	37.9	30.9

Table 2: Overall value and fundamental component of pressure ripple at a pump exit

			Low speed (920 rpm)			High speed (2.000 rpm)		
			Fixed	Var-C	Var-M3	Fixed	Var-C	Var-M3
Pressure ripple[dB]	Overall	Low pressure (0.7 MPa)	-19.8	-15.2	-15.2	-15.4	-15.2	-16.2
		High pressure (5.4 MPa)	-8.3	-4.0	-9.3	-4.4	-2.6	-6.3
	Fundamental	Low pressure (0.7 MPa)	-37.1	-26.4	-43.9	-17.0	-20.7	-23.7
		High pressure (5.4 MPa)	-17.4	-8.3	-21.3	-6.9	-10.7	-12.3

From these experimental results, the following can be seen. The reduction in overall sound pressure level by using the Var-M3 pump is only 1.2 dB on average compared to that of the Var-C pump (almost same level compared to that of the fixed pump). However, the fundamental component of the sound pressure level, which has a great influence on the tone quality of noise, can be reduced by around 9 dB and 4 dB compared to the Var-M3 pump and fixed pump, respectively. As being pointed out by Christian et al (1999), it is noticeable to recall that for noise, vibration and harshness, the harmonic composition of the pump signature is a significant factor rather than the overall level. The Var-M1 - Var-M3 pumps have been highly praised also by a sensorial test by a jury of engineers.

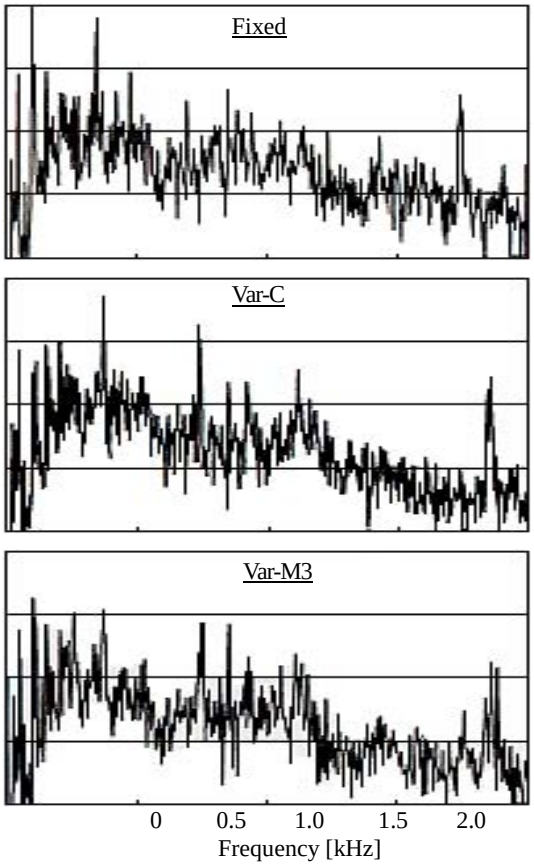

Fig. 12: *Spectra of A-weighted sound pressure level in a passenger compartment (N = 2000 rpm, P_d = 5.4 MPa)*

Furthermore, it was found that there was a good correlation between the harmonic component of the pressure ripple and the sound pressure level, and thus the noise in a passenger compartment is mainly caused by a pressure ripple due to pump source flow ripple (i.e., by a fluid-borne noise).

6 Conclusions

The main results of this study are summarized as follows.

1. The excessive increase in fluid-borne noise produced by an existing variable-displacement vane pump equipped with a conventional cylindrical cam ring is mainly caused by the increase in intermittent unsteady vane tip leakage due to vane bounce occurring in the trapping section near the bottom dead center.

2. The variable-displacement vane pump equipped with this devised "modified profile cam ring" (MPCR) can reduce the pump source flow ripple and then the pressure ripple in the pressure line to at least the level of a fixed-displacement pump over a wide range of operating conditions.
3. The variable-displacement vane pump equipped with the MPCR is greatly effective especially on the improvement of sound quality of noise in a passenger compartment of a real car, and some types of them have already been put into practice in several kinds of automobiles in Japan. Further, this invention has acquired United States Patent (Patent No.: US 6,503,068 B2, Date of Patent: 7. January 2003) as well as Japanese Patent.

Acknowledgement

The author gratefully acknowledges the assistance of Y. Toshimitsu, C. Wang and K. Ando of SHOWA Corporation (Japan) and S. Ogura (graduate student) of Kanagawa University.

Nomenclature

A_d	orifice area of discharge port	[m^2]
A_s	orifice area of suction port	[m^2]
A_v	orifice area over vane tip during vane bounce	[m^2]
B	fluid bulk modulus	[Pa]
B_e	effective fluid bulk modulus in vane chamber	[Pa]
C_d	orifice flow coefficient	[-]
e	eccentric distance of rotor	[m]
N	pump revolution speed	[rpm]
P_0	atmospheric pressure	[Pa]
P_d	mean discharge pressure	[Pa]
P_s	mean suction pressure	[Pa]
P_t	pressure in vane chamber near bottom and top dead center	[Pa]
P_t*	absolute pressure of P_t	[Pa]
Q_a	actual pump delivery flow	[m^3/s]
Q_{cd}	inlet flow at discharge port	[m^3/s]
Q_{cs}	inlet flow at suction port	[m^3/s]
Q_{cv}	leakage over vane tip during vane bounce	[m^3/s]
Q_{th}	kinematic flow	[m^3/s]
ΔQ_{tb}	unsteady leakage near bottom dead center	[m^3/s]
ΔQ_{tt}	unsteady leakage near top dead center	[m^3/s]
ΔQ_l		[m^3/s]
$R(\beta)$	radius of curvature of cam ring	[m]
$r(\phi)$	radius vector of vane	[m]
$r_0(\phi)$	radius vector of vane of design objective	[m]
t	time	[s]
V_i	ith vane chamber volume in discharge stroke	[m^3]
V_t	vane chamber volume near bottom and top dead center	[m^3]
κ	ratio of specific heats for air	[-]
β	cam ring angular position relative to bottom dead center	[rad]
ϕ	rotor angular position relative to bottom dead center	[rad]
θ	angular position of center between two adjacent vanes	[rad]
χ_0	ratio of air/fluid volume	[-]

References

Dickinson, L. A., Edge, A. K. and **Johnston, N. D.** 1993. Measurement and Prediction of Power Steering Vane Pump Fluidborne Noise. *SAE Technical Paper Series* 931294, pp. 267-275.

Bleitz, D., Fernholz, C. and **Ivkovich, S.** 1997. Automated Production Noise Testing of Power Steering Pumps. *SAE* 971911, *SAE Noise and Vibration Conference and Exposition*, Traverse City, Michigan.

Karmel, M. A. 1986. A Study of the Internal Forces in a Variable-Displacement Vane-Pump-Part: l, A theoretical Analysis. *ASME Journal of Fluid Engineering*, Vol. 108, No. 2, pp. 227-232.

Karmel, M. A. 1986. A Study of the Internal Forces in a Variable-Displacement Vane-Pump-Part: ll, A Parametric Study. *ASME Journal of Fluid Engineering*, Vol. 108, No. 2, pp. 233-237.

Kojima, E. 1992. A new method for the experimental determination of pump fluid-borne noise characteristics. *Fifth Bath International Fluid Power Workshop 1992*, Bath, U.K., pp. 111-137.

Kojima, E., Yu, J. and **Ichiyanagi, T.** 2000. Experimental Determination and Theoretical Predicting of Source Flow Ripple Generated by Fluid Power Piston Pump. *SAE Technical Paper Series* 2000-01-2617, pp. 1-9.

Fernholt, M. C. and **Bishop, F. L.** 1999. Use of Binaural Measurement and Analysis Techniques in the Establishment of Steering Pump Design Tolerances for Noise, Vibration and Harshness Performance. *SAE Technical Paper Series* 1999-01-1852, pp. 1-6.

Qatu, S. M., Dougherty, L. M. and **Llewllyn, R. D.** 1999. Repeatability of Impedance and Ripple Tests for automotive Pumps. SAE 99NV-219. *SAE Noise and Vibration Conference and Exposition*, Traverse City, Michigan.

Appendix

An outline of the numerical calculation procedures of source flow ripple produced by a variable-displacement vane pump equipped with a proposed "modified profile cam ring" (MPCR) is given here under.

Actual delivery flow rate from the pump, Q_a, is given by,

$$Q_a = Q_{th} - \Delta Q_{tb} - \Delta Q_{tt} - \Delta Q_l \quad \text{(A1)}$$

where, Q_{th} is the theoretical (neglecting leakage) flow-rate determined by the pump geometry and pump revolution speed, ΔQ_{tb} and ΔQ_{tt} the unsteady leakage flow rate near the bottom and top dead centers, respectively, and ΔQ_l the steady leakage flow rate (such as a leakage at the rotor sides).

Applying the continuity equation to the control volume in Fig. 13 yields the governing equation for unsteady leakage flow rate, ΔQ_{tb}, and fluid chamber pressure, P_t.

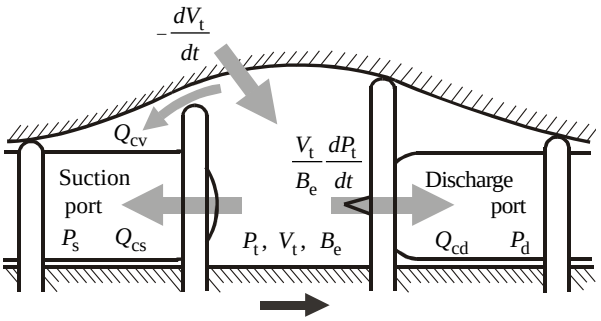

Fig. 13: *Schematic illustration showing vane chamber flows nearby dead centers*

$$\Delta Q_{tb} = \frac{V_t}{B_e}\frac{dP_t}{dt} + Q_{cs} + Q_{cv} = -\frac{dV_t}{dt} - Q_{cd} \quad \text{(A2)}$$

$$\frac{dP_t}{dt} = \left(-Q_{cd} - Q_{cs} - Q_{cv} - \frac{dV_t}{dt}\right)\frac{B_e}{V_t} \quad \text{(A3)}$$

B_e in Eq. A2 and A3 is the effective fluid bulk modulus that takes the effect of entrained free bubbles in the fluid into consideration, given by;

$$B_e = \frac{B}{1 + x_0(B/\kappa P_t - 1)(P_0/P_t)^{1/\kappa}} \quad \text{(A4)}$$

where, B is the bulk modulus of fluid excluding entrained air, χ_0 the ratio of air/fluid volume at atmospheric pressure P_0 (abs.), κ the ratio of specific heat for air, and P_t* the absolute pressure of P_t. An orifice flow equation is used to determine the flow rate through the discharge port and suction port from the vane chamber, Q_{cd}, and Q_{cs}, respectively, and the leakage flow rate over the vane tip during vane bounce, Q_{cv}.

$$Q_{cd} = \text{sign}(P_t - P_d) C_d A_d(\theta) \sqrt{2|P_t - P_d|/\rho} \quad \text{(A5)}$$

$$Q_{cs} = \text{sign}(P_t - P_s) C_d A_s(\theta) \sqrt{2|P_t - P_s|/\rho} \quad \text{(A6)}$$

$$Q_{cv} = \text{sign}(P_t - P_s) C_d A_v(\theta) \sqrt{2|P_t - P_s|/\rho} \quad \text{(A7)}$$

For the variable-displacement vane pump equipped with a cylindrical cam ring, Q_{th} , V_t and dV_t/dt in Eq. A1 - A3 can be obtained in the form of analytical solutions. However, for the pump equipped with the MPCR, these values cannot be obtained analytically because the radius of curvature of the cam ring is given through numerical data. In this study, these values for such a pump were calculated numerically as follows.

(i) Volume of vane chamber, V_t , and rate of its change respect to time, dV_t/dt

Figure 14 shows the relationship between the radius vector of the vane and the radius of curvature of the cam ring. First, the radius of curvature of the cam ring, $R(\beta)$, is calculated from the following equation based on the numerical data of the radius vector of the vane, $r_0(\phi)$, at eccentricity of e_0 (shown in Fig. 8), which is specified as a design value.

$$R = \sqrt{r_0^2 + e_0^2 - 2r_0 e_0 \cos\phi} \quad \text{(A8)}$$

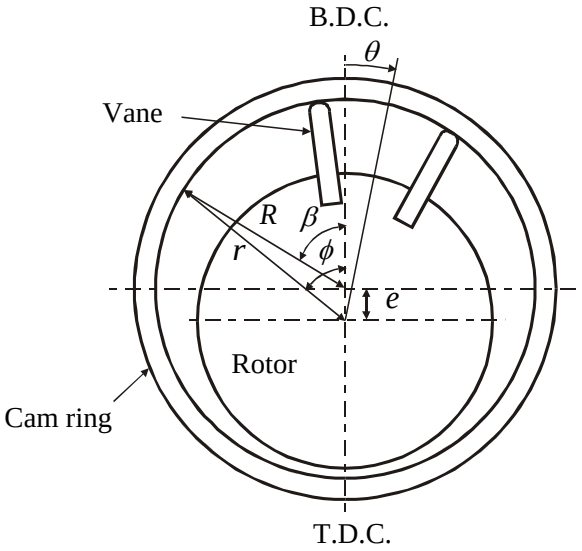

Fig. 14: *Relation between radius vector of vane and radius of curvature of cam ring profile*

$$\beta = \tan^{-1}\left(\frac{r_0 \sin\phi}{r_0 \cos\phi - e_0}\right) \quad \text{(A9)}$$

Next, the value of R at every 1° interval of β over the range of 360° is calculated from $R(\beta)$ obtained above (and then is input to the NC cam grinding machine). Once the radius of curvature of the cam ring is determined, the relationship between the radius vector of the vane, r, and the rotational angle of the vane, ϕ, at any eccentricity, e, can be obtained by the following equations.

$$R = \sqrt{R^2 + e^2 - 2Re\cos\beta} \quad \text{(A10)}$$

$$\phi = \tan^{-1}\left(\frac{R\sin\beta}{R\cos\beta + e}\right) \quad \text{(A11)}$$

Provided that, in this simulation analysis, the value of R between every 1° interval of β is obtained by the approximation of linear interpolation. Lastly, V_t and dV_t/dt at any time, t, and any eccentricity, e, are calculated using Eq. A10 and A11.

(ii) Theoretical pump delivery flow rate

The theoretical delivery flow rate due to only the pumping mechanism, $Q_{th,}$ is the total sum of volume change-rate of vane chambers ($-dV_i/dt$) existing in a discharge stroke and obtained by Eq. A12. Provided that

both ends of the suction and delivery ports of the modified profile cam ring in theory are supposed to be located so that the dead centers come to the angular position that satisfies $dV_t/d\theta = 0$.

$$Q_{th} = \sum_{i=1}^{K}\left(-\frac{dV_i}{dt}\right) \qquad \text{(A12)}$$

where, k is the number of vane chambers located in a discharge stroke. The present calculation method can also be applied to the cylindrical cam ring by using $R(\beta)$ of constant value of course.

Eiichi Kojima
(Born 14th May 1937) is Professor of Kanagawa University in Japan. He completed the postgraduate course of University of Tokyo and received his Dr. Eng. degree in 1969. His research interests include noise- vibration-harshness of hydraulic components and systems, optimum design, and simulations. He has won prizes of best paper of Transaction JHPS in the 1997 and 1999 fiscal year. Since 1996 he has acted as a Japanese expert of the ISO TC131/SC8/WG1.